This article has been accepted for publication in a future issue of this journal, but has not been fully edited. Content may change prior to final publication.
Citation information: DOI: 10.17775/CSEEJPES.2021.00510, CSEE Journal of Power and Energy Systems

Moisture Evaluation of Oil-immersed Insulation in Bushing Based on Frequency Domain Spectroscopy and Grey Relational Analysis

Xianhao Fan, *Student Member, IEEE*, Sheng Li, Tengyue Sun, Yiyi Zhang*, *Member, IEEE*, and Jiefeng Liu, *Member, IEEE*

***Abstract*—Operation level and service life of oil-immersed bushing are related to the moisture inside its cellulose insulation. However, the parameters extracted by using existing frequency domain spectroscopy (FDS) based methods strongly depend on the data within a certain range or several sampling points, which could decrease the accuracy of extraction results if the measured FDS data is unreliable in the above region. Given this issue, a universal and accessible tool is proposed to stimulate the change rule of FDS curves versus entire frequency regions, by which a set of feature parameters can be readily obtained by using Taylor series model. Then, the database characterizing the moisture is established. An alternative method for evaluating the moisture in bushing cellulose insulation is proposed based on FDS and grey relational analysis (GRA). The feasibility and applicability of the proposed method were later proved by the moisture evaluation of transformer oil-immersed bushing, in which the GRA is applied as a tool for moisture classification. The results showed that the average relative (absolute error) is less than 14.6 %(0.17 %). Thus, the proposed method could be preliminarily utilized for evaluating the moisture inside the bushing cellulose insulation.**

***Index Terms*—Transformer bushing, Oil-immersed cellulose insulation, Frequency domain spectroscopy (FDS), Moisture evaluation**

I. Introduction

OIL-IMMERSED bushing is one of the core components related to power transformers, whose fault might directly lead to the accident of transformers [1]-[3]. The fault proportion caused by cellulose insulation inside oil-immersed bushing in total accidents increased with the prolonged service record of these transformers [4].

In order to avoid the unnecessary economic loss caused by the accident of the oil-immersed bushing, the available and reliable evaluation method of cellulose insulation in the oil-immersed bushing is thus of great interest to scholars [5]-[8]. The insulation performance of bushing is reduced by moisture, which is attributed to two main factors. On the one hand, the moisture is identified as an aging by-produce, which will be accumulated with the prolonged operation duration and deepened degradation of cellulose insulation [9], [10]. On the other hand, external moisture will intrude into the insulation system during maintenance, fault, and even normal operation. By virtue of the inside moisture is capable of decreasing the electric strength (by means of decreasing the breakdown voltage), as well as aggravating the aging reaction of cellulose insulation [11], [12]. Consequently, moisture is considered an important factor that affects the insulation conditions and service life of the oil-immersed bushing. Thus, the necessary attention is needed to be paid to the accident caused by moisture inside the oil-immersed bushing.

Reviewing the existing research, the traditional methods based on the test of insulation resistance and insulation capacitance contain insufficient insulation information, which leads to difficulty in the evaluation of both aging degree and moisture by using such limited information [14]. Besides, the dissolved gas analysis (DGA) in oil-immersed bushing needs to access oil samples from the bushing, which will destroy the sealing performance of the bushing [15], by which the moisture and oxygen in the air will invade the bushing and leads to degradation. Thus, the traditional methods for evaluating the conditions of the bushing insulation need further development. Because of the non-destructive property, anti-interference performance, and rich insulation information, the frequency domain spectroscopy (FDS) based methods have been adopted by researchers to perform the same research [16], [17].

Compared with the traditional method, the FDS based method could access more information for characterizing the insulation states without any sampling damage. Therefore, various FDS based researches for moisture analysis of oil-immersed cellulose can be found [6], [18]-[20]. The two manners of moistening on oil-immersed bushing were introduced in [19], in which the dielectric response characteristics under different moisture, as well as different moistening manners, have been also analyzed. Further, the nonlinear phenomenon of bushing FDS test with different moisture was observed by experiment in reference [20, 21], and the feature parameters (extracted by using the dielectric loss curve) and quantitative method of *mc%* of bushing were obtained as well. From literature [6], the influence of different

Manuscript received Jan 18, 2021; revised Feb 20, 2021; accepted May 26, 2021. Date of online publication April ××, 2022; date of current version ×× ××, 2022. This work was supported in part by the National Natural Science Foundation of China under Grant 51867003, and in part by the Natural Science Foundation of Guangxi under Grant 2018JJB160064 and 2018JJA160176, and in part by Guangxi Key Laboratory of Power System Optimization and Energy Technology Project under Grant AE3020001829. (Corresponding author: Yiyi Zhang)

X. H. Fan, S. Li, T. Y. Sun, Y. Y. Zhang, J. F. Liu are with the School of Electrical Engineering, Guangxi University, Nanning, China (e-mail: xianhao_fan@163.com, sheng_li@st.gxu.edu.cn, 1912301048@gxu.edu.cn, yiyizhang@gxu.edu.cn, jiefengliu2018@gxu.edu.cn).

Digital Object Identifier:

mc% inside the bushing on the FDS curves was studied, then, the relationship between relevant feature parameters (dielectric dissipation integral factor) and moisture was obtained. However, such a relationship has not been used to evaluate the bushing with unknown moisture. However, the extracted parameters strongly depend on the FDS data of a certain measurement point or a range, which could decrease the accuracy of extraction results if the measured data in such a point or range is unreliable.

Given these issues, this work proposed an alternative method for evaluating the moisture in bushing based on the FDS and the Grey Relational Analysis (GRA) [22]. In the current work, a universal and accessible tool to stimulate the change rule of dielectric loss versus entire frequency regions, by which a set of feature parameters for characterizing the inside moisture can be readily obtained by using Taylor series [23]. The quantitative relation of the feature parameters versus the moisture was studied by using the fitting analysis, which could help to develop a parameters database. Finally, based on the developed parameter database and GRA, the feasibility and applicability of the proposed method are verified with the moisture evaluation of the three transformer bushings. The results revealed that the average relative error (absolute error) between the evaluated moisture and the tested value of three transformer bushings is less than 14.6 % (0.17 %). Therefore, the proposed method could provide an alternative approach for evaluating the moisture inside the bushing cellulose insulation.

II. Mathematical Model of FDS Technique

A. Fundamental Theory

During the FDS test, the applied alternating electric field $E(\omega)$ can be expressed as follows.

$$E(\omega) = E_m e^{j\omega \cdot t} \tag{1}$$

Where ω is the angular frequency, j is the sign of the imaginary part, E_m is the amplitude of the electric field, and t is the time. Under the motivation of $E(\omega)$, the polarization process could be built, then, the electric displacement $D(\omega)$ can be described by using (2).

$$D(\omega) = D_m e^{j(\omega t - \delta)} \tag{2}$$

Where, δ is the angle behind the $E(\omega)$ when the polarization begins to establish. The D_m is the amplitude of electric displacement. Then, the $\varepsilon^*(\omega)$ can be obtained.

$$\begin{aligned} \varepsilon^*(\omega) &= \frac{D(\omega)}{\varepsilon_0 E(\omega)} = \frac{D_m(\omega)}{\varepsilon_0 E_m(\omega)} \cdot e^{-j\delta} \\ &= \varepsilon'(\omega) - j\varepsilon''(\omega) \end{aligned} \tag{3}$$

The $\varepsilon_r'(\omega)$ and $\varepsilon_r''(\omega)$ are the real and imaginary parts of the $\varepsilon_r^*(\omega)$. The relationship between $\varepsilon^*(\omega)$ and relative complex permittivity $\varepsilon_r^*(\omega)$ is expressed by (**4**).

$$\varepsilon_r^*(\omega) = \frac{\varepsilon^*(\omega)}{\varepsilon_0} \tag{4}$$

Then, the polarization current density $J(\omega)$ that flows through the dielectric insulation can be obtained.

$$J(\omega) = E(\omega)\varepsilon_0 j\omega \cdot [\varepsilon'(\omega) + j\varepsilon_r''(\omega)] \tag{5}$$

In Equation (**5**), $j\omega E(\omega)\varepsilon_0\varepsilon_r'(\omega)$ represents the reactive current, while $\omega E(\omega)\varepsilon_0\varepsilon_r''(\omega)$ represents the active current. Then, the dielectric loss tan $\delta(\omega)$ can be obtained by (**6**).

$$\begin{aligned} \tan\delta(\omega) &= \frac{\omega E(\omega)\varepsilon_0\varepsilon_r''(\omega)}{\omega E(\omega)\varepsilon_0\varepsilon_r''(\omega)} \\ &= \frac{\varepsilon_r''(\omega)}{\varepsilon_r'(\omega)} \end{aligned} \tag{6}$$

B. Mathematical Model of Dielectric Loss Based on Taylor Series Model

Various relaxation and conductance processes would be established during the dielectric response process [24]. When we plotted the measured dielectric loss tan δ as a continuous curve in a certain frequency range, its change period can be assumed to be infinite, also, any point on the curve can be derived. Then, the Taylor series can be used to approximate such a continuous curve.

If $G(f)$ is presumed as the function of tan $\delta(\omega)$, $G(f)$ can be considered as a continuous curve, which is constituted by various sub-curves. In this case, the Taylor series [23] can be utilized to describe such phenomena, as is shown in (**7**).

$$\begin{aligned} G(f) = G(f_0) &+ \frac{G'(f_0)}{1!}(f-f_0) + \frac{G''(f_0)}{2!}(f-f_0)^2 \\ &+ \cdots + \frac{G^{(n)}(f_0)}{n!}(f-f_0)^n \end{aligned} \tag{7}$$

Where, f_0 is a constant, $f_0 \in (2\times10^{-4},\ 5\times10^{3})$. $G^{(n)}(f_0)$ represents the n-order derivative of $G(f)$ when $f=f_0$, in this case, $G^{(n)}(f_0)$ is also a constant. The feature parameter A_i (i=1, 2, …, n) is then introduced:

$$\begin{cases} G(f_0) = A_0 \\ G'(f_0)/1! = A_1 \\ \quad\vdots \\ \dfrac{G^{(n)}(f_0)}{n!} = A_n \end{cases} \tag{8}$$

By substituting Equation (**8**) into (**7**), Equation (**9**) can be obtained.

$$G(f) = A_0 + A_1(f-f_0) + A_2(f-f_0)^2 + \cdots + A_n(f-f_0)^n \tag{9}$$

According to Equation (**10**), eliminating all parentheses in Equation (**9**), and merging sub-terms of variable f with the same order, Equation (**11**) is later obtained.

$$[f + (-f_0)]^n = \sum_{r=0}^{n} C_n^m \cdot f^{n-m} \cdot (-b)^m \tag{10}$$

$$\begin{aligned} G(f) = A_0 &- f_0 \cdot A_1 + \frac{2!}{2!} f_0^2 \cdot A_2 + \cdots + \frac{n!}{n!}(-f_0)^n \cdot A_n \\ &+ [A_1 - \frac{2!}{1!} f_0 \cdot A_2 + \cdots + \frac{n!}{(n-1)!} \cdot (-f_0)^{n-1} \cdot A_n] \cdot f \\ &+ [A_2 - \frac{3!}{1!\,2!} f_0 \cdot A_3 + \cdots + \frac{n!}{(n-2)!\,2!} \cdot (-f_0)^{n-2} \cdot A_n] \cdot f^2 \\ &+ \cdots + A_n \cdot f^n \end{aligned} \tag{11}$$

The coefficients of f^n(n=0, 1, 2 …) are then merged and represents by using Λ_i (i=1,2,…,n). The expression of Λ_i is shown in Equation (**12**).

Citation information: DOI: 10.17775/CSEEJPES.2021.00510, CSEE Journal of Power and Energy Systems

$$\begin{cases} \Lambda_0 = A_0 - f_0 \cdot A_1 + \dfrac{2!}{2!} f_0^2 \cdot A_2 + \cdots + \dfrac{n!}{n!}(-f_0)^n \cdot A_n \\ \Lambda_1 = A_1 - \dfrac{2!}{1!} f_0 \cdot A_2 + \cdots + \dfrac{n!}{(n-1)!} \cdot (-f_0)^{n-1} \cdot A_n \\ \Lambda_2 = A_2 - \dfrac{3!}{1!\,2!} f_0 \cdot A_3 + \cdots + \dfrac{n!}{(n-2)!\,2!} \cdot (-f_0)^{n-2} \cdot A_n \\ \vdots \\ \Lambda_n = A_n \end{cases} \tag{12}$$

Finally, Equation (**13**) can be obtained by substituting (**12**) into (**11**).

$$\begin{aligned} G(f) &= \Lambda_0 + \Lambda_1 f + \Lambda_2 f^2 + \cdots + \Lambda_n f^n \\ &= \sum_{i=0}^{n} \Lambda_i \cdot f^i \quad (i = 1, 2, ..., n) \end{aligned} \tag{13}$$

Equation (**13**) can be written as follow when including the moisture impact. Where, only the single independent variable f is contained in the equations, the $\Lambda_i(mc\%)$ would be affected by the inside moisture content.

$$\tan\delta(f) = G(f) = \sum_{i=0}^{n} \Lambda_i(mc\%) \cdot f^i \quad (i = 1, 2, ..., n) \tag{14}$$

III. Experimental Platform for Sample Preparation and Test

A. Preparation of Insulation Pressboards with Various Moisture

The 25# mineral insulating oil (pour point≤-45 ℃, flash point is 135 ℃) manufactured by Chuanrun Petrochemical Co. Ltd. and T4 disc pressboard (thickness: 0.5 mm; density: 0.96 g/cm^3; diameter: 160 mm) manufactured by Taizhou Weidmann High Voltage Co. Ltd. were used to prepare the oil-immersed cellulose samples. Before the experiment, the pressboard and oil were dried in vacuum for 48h, at 105 ℃/50 Pa, respectively. The moisture content (*mc*%) of the pretreated pressboard should be less than 1 %. Besides, in order to simulate the generated moisture gradient in bushing after a long-time operation, six moisture levels were considered in the experiments on moisture absorption. Also, since the *mc*% inside cellulose insulation in some bushing will even close to or exceeds 4 % with the increasing operation duration, the maximum value of *mc*% in this work is close to 4 % as well.

Then, the pressboards with various moisture were immersed in insulation oil at 60 ℃/50 Pa, and balanced for 48h before the FDS test. The details of the preparation and measurement of oil-immersed cellulose samples with various moisture can be described using Fig. **1** [9].

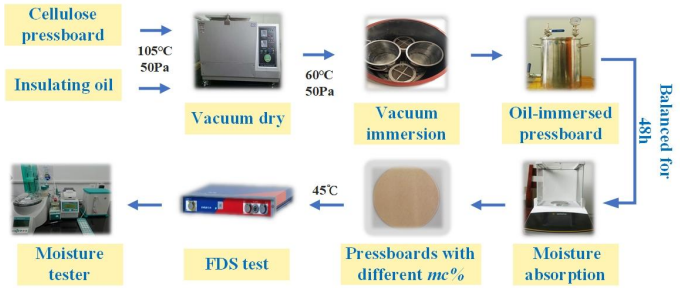

Fig. 1. Experiment scheme of sample preparation and FDS test.

B. FDS Test and Moisture Measurement of Prepared Cellulose Samples

According to the literature [25], the influence of aluminum foil contained in the capacitor core of bushing on measured FDS data would be ignored when constructing the experimental model. Therefore, in this work, the prepared oil-immersed samples without aluminum foil are chosen for the FDS test.

The FDS test was launched under 45℃ in lab conditions by using a dielectric response tester (DIRANA/OMICRON) and the three-electrode test cell. The measured frequency region is 2×10^{-4} to 5×10^{3} Hz, the test temperature is 45 ℃ [17]. In order to ensure the repeatability of the test, the test activity on each sample will be performed three times, and the obtained average value is regarded as the final result. According to the recorded results, the average value of the standard deviation of 18 (3×6) measurements is equal to 1.57E-2.

According to Fig. **1**, six groups of samples with different *mc*% were tested under lab conditions, and their tan $\delta(\omega)$ are shown in Fig. **2**. From Fig. **2**, the moisture of samples was tested by using Coulomb Karl Moisture Tester (831+885) based on standard IEC 60814, which is sequentially equal to 0.73 %，0.91 %，1.31 %，2.47 %，3.24 %, and 3.84 %. The test scheme is shown in Fig. **3**.

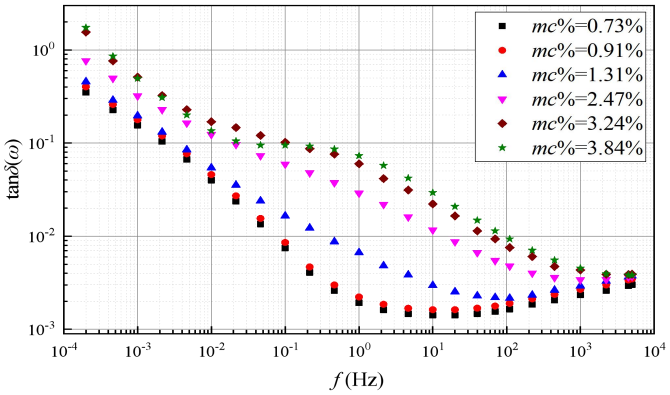

Fig. 2. The tan$\delta(\omega)$ curves of prepared samples with different *mc*%.

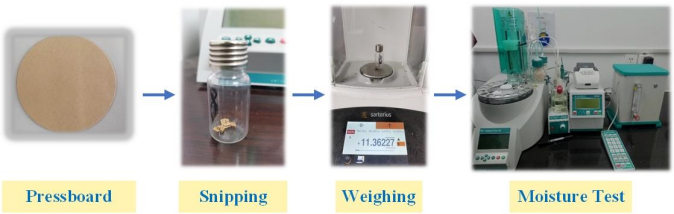

Fig. 3. The test scheme of the moisture inside the cellulose samples.

C. Establishment of Parameter Database

1) Extraction of feature parameters by using Taylor series model

From Fig. **3**, it can be found that the shape of tan $\delta(\omega)$ curves of samples with different moisture is distinct. Furthermore, each curve tends to move to a higher frequency region with an increase of *mc*%. However, the moisture impact on tan $\delta(\omega)$ curves can be only qualitatively analyzed with observation. While, if we want to quantify such moisture impact as accurately as possible, the corresponding feature parameters, sensitive to the moisture impact, could be extracted to achieve this goal.

In relation to this assumption, (**11**) could be effectively used for extracting these feature parameters, in which the contained parameters Λ_i (i = 1, 2, 3, ..., n) is exactly what we wanted. It should be noted that the fitting goodness of the measured tan$\delta(\omega)$ by using (**11**) is always determined by the value of defined n in the formula. Specifically, the higher the n, the greater the fitting goodness. Nevertheless, the uncertainty could be also brought when using a high value of n. Therefore, it is important to choose a reasonable value of n. Fig. **4** plotted the comparison of the fitting results when n=3 to 5 respectively.

Then, it is found that the fitting goodness under the condition of n=4 is higher than the n=3. The R^2 does not increase sharply when n=5, while the complexity of fitting analysis increased with the increasing n. Thus, n=4 is satisfactory for performing the corresponding fitting analysis in this work.

In view of this, (**11**) (when n = 4) was selected. Therefore, the FDS test results, i.e. tan$\delta(\omega)$, can be transformed from 'graphical' to 'digital' by using (**11**). The feature parameters and their fitting goodness R^2 of tan$\delta(\omega)$ of samples with different mc% are shown in Table **I**.

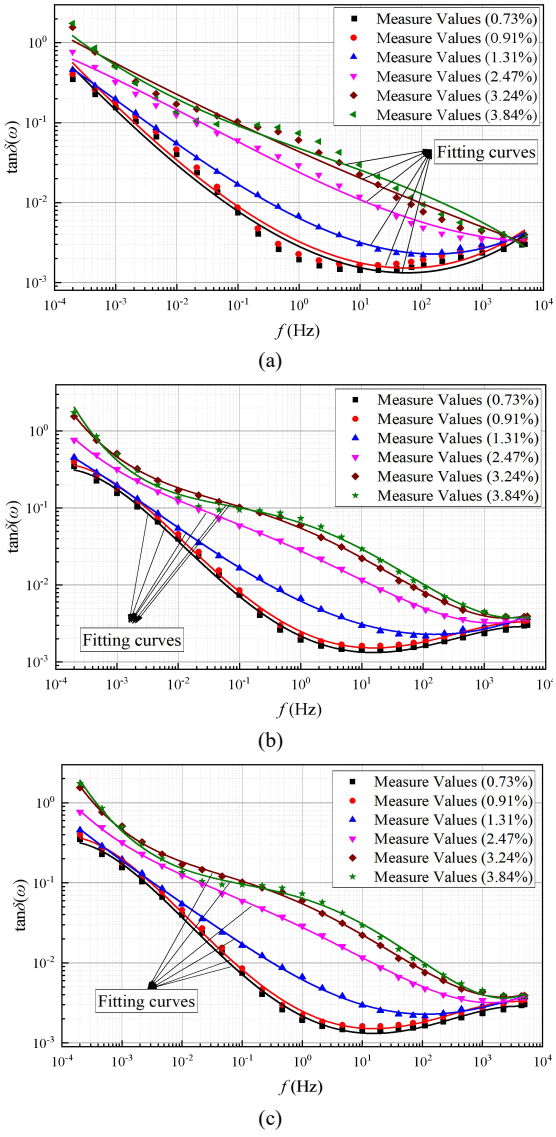

Fig. 4. The comparison of the fitting results by using (**11**).
(**a**) n=3, (**b**) n=4, (**c**) n=5.

TABLE I
EXTRACTED FEATURE PARAMETERS UNDER DIFFERENT mc%

mc%	Feature parameters					R^2
	Λ_0	Λ_1	Λ_2	Λ_3	Λ_4	
0.73 %	-2.66353	-0.3695	0.15894	0.00690	-0.00553	0.998
0.91 %	-2.60331	-0.36976	0.15881	0.00692	-0.00552	0.998
1.31 %	-2.20919	-0.37442	0.06774	0.00706	-0.00050	0.999
2.47 %	-1.5563	-0.36334	-0.02337	0.00361	0.00331	0.999
3.24 %	-1.26073	-0.33206	-0.05831	-0.00137	0.00516	0.999
3.84 %	-1.19243	-0.26108	-0.07882	-0.00779	0.00653	0.997

2) Parameters Extraction by using Taylor series model

In the previous section, the feature parameters under 6 kinds of mc% are extracted. However, if only use these parameters to evaluate the moisture condition of the bushing, an obvious error would be generated since the evaluation precision is insufficient. Besides, on the condition that the mc% of the bushing is more than 3.84 %, or less than 0.73 %, the developed evaluation method will be not suitable.

For overcoming the above difficulties, this part tries to determine the relationship between the extracted feature parameters and mc% by using the fitting analysis. According to Λ_i in Table **I**, with the increase of mc%, the value of Λ_i meets the exponential growth or decay law. Therefore, the exponential fitting model is utilized to fitting the Λ_i versus mc%. The obtained fitting equation can be used as an effective way to calculate the Λ_i under different mc%. The detailed information of the fitting equation is shown in Table **II**, and the fitting curves are shown in Fig. **5**.

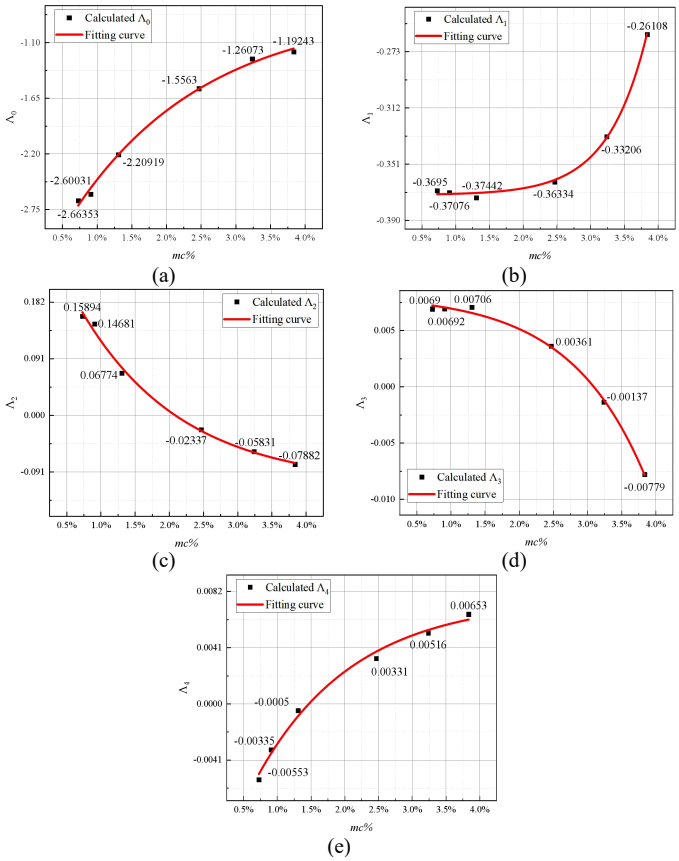

Fig. 5. Fitting curves of feature parameters versus moisture.
(**a**) Λ_0, (**b**) Λ_1, (**c**) Λ_2, (**d**) Λ_3, (**e**)Λ_4.

Citation information: DOI: 10.17775/CSEEJPES.2021.00510, CSEE Journal of Power and Energy Systems

TABLE II
FITTING EQUATIONS OF FEATURE PARAMETERS VERSUS MOISTURE

Used formula	$\Lambda_i(mc\%) = a \cdot EXP(mc\%/t) + y$			R^2
Parameters	*a*	*t*	*y*	
Λ_0	-2.83211	-1.93078	-0.77214	0.996
Λ_1	-0.00015	0.57841	-0.37259	0.998
Λ_2	0.45218	-1.48354	-0.11096	0.995
Λ_3	-0.00050	1.10754	0.00819	0.998
Λ_4	-0.02115	-1.44213	0.00761	0.993

3) Establishment of feature parameters database

Referring to the fitting equations shown in Table **II**, the feature parameters corresponding to any *mc*% can be readily calculated. Thus, if we want to improve the evaluation precision, the database formed by feature parameters corresponding to the many moistures is firstly needed to develop, by which the dielectric response property under various moisture could be also quantified with these calculated feature parameters contained in this database. The steps are as follows. Firstly, the available *mc*% range of the database should be confirmed. During the manufacturing process of the transformer (including bushing), the cellulose insulation system will be dried, and the *mc*% of cellulose insulation is generally controlled at about 0.5 %. Besides, as mentioned in the previous section, the *mc*% inside cellulose insulation in some bushing could exceed 4 % with the increasing service duration. Given this, the minimum and maximum values of *mc*% used in the database are set to 0.5 % and 4.5 %.

Secondly, the altering step of *mc%* within the defined available range should be also confirmed. The evaluation precision is directed related to the defined altering step. Specifically, the smaller the altering step, the richer the feature parameter characterizing the diverse moisture. However, if the altering step is selected too small, it will dramatically increase the difficulty and time required for evaluation. Besides, it can be expected that the precision will be difficult to significantly increase when the altering step is small enough. Thus, according to repeat verification, the altering step of moisture preset to 0.2 %, which can be expressed as follow.

$$mc\%_j = 0.5\% + 0.2\% \cdot j \tag{15}$$

Where, *j* is the number of the preset moisture, and *j*= 0, 1, …, 20. Then, the feature parameter database will be established according to the following steps.

a. The present $mc\%_i$ is calculated by using (**12**).

b. Substituting the calculated *mc*% into the fitting equations shown in Table **II**, then, the corresponding feature parameters (Λ_i) will be obtained.

b. The formed database contains 21 sets of feature parameters and are shown in Table **III**.

TABLE III
THE FEATURE PARAMETERS DATABASE

Moisture	Feature parameters				
	Λ_0	Λ_1	Λ_2	Λ_3	Λ_4
0.5%	-2.95810	-0.37224	0.21184	0.00740	-0.00734
0.7%	-2.74300	-0.37210	0.17113	0.00724	-0.00541
0.9%	-2.54907	-0.37190	0.13555	0.00706	-0.00372
1.1%	-2.37422	-0.37161	0.10446	0.00683	-0.00225
1.3%	-2.21657	-0.37121	0.07729	0.00656	-0.00098
1.5%	-2.07444	-0.37064	0.05355	0.00624	0.00013
1.7%	-1.94629	-0.36983	0.03280	0.00586	0.00110
1.9%	-1.83075	-0.36869	0.01467	0.00540	0.00194
2.1%	-1.72658	-0.36707	-0.00117	0.00485	0.00267
2.3%	-1.63267	-0.36480	-0.01502	0.00419	0.00331
2.5%	-1.54799	-0.36158	-0.02712	0.00340	0.00387
2.7%	-1.47164	-0.35703	-0.03769	0.00245	0.00435
2.9%	-1.40281	-0.35060	-0.04693	0.00132	0.00477
3.1%	-1.34075	-0.34151	-0.05501	-0.00004	0.00514
3.3%	-1.28480	-0.32867	-0.06207	-0.00167	0.00546
3.5%	-1.23435	-0.31053	-0.06823	-0.00362	0.00574
3.7%	-1.18887	-0.28490	-0.07362	-0.00596	0.00598
3.9%	-1.14786	-0.24867	-0.07833	-0.00876	0.00619
4.1%	-1.11089	-0.19748	-0.08245	-0.01211	0.00637
4.3%	-1.07756	-0.12515	-0.08604	-0.01613	0.00653
4.5%	-1.04750	-0.02293	-0.08918	-0.02095	0.00667

IV. FEASIBILITY VERIFICATION OF THE PROPOSED METHOD

In previous sections, the feature parameter database for characterizing the moisture inside the oil-immersed insulation has been constructed. Then, a classification model, such as one devoted to comparing the similarity, is needed to complete the moisture evaluation. Therefore, the GRA is introduced to perform the moisture evaluation of the bushing insulation.

A. Grey Relational Analysis Model

The Grey Relational Analysis (GRA) focuses on the degree of correlation (similarity) between several discrete functions to one discrete function [21-22]. This model is utilized since it has the advantages of simple principle, convenient calculation, and short time-consuming. Besides, researchers only need to calculate the correlation coefficient to get the correlation degree, and then get the similarity between the unknown samples and the known samples according to the correlation degree. The detailed steps are as follows.

Step 1: Define the data array formed by feature parameters is $X_k(\Lambda_{k,r})$, when *k*=0, the array is defined as the evaluation array of the unknown sample, while the array will be defined as the reference array of the known sample when *k*=1, 2, …21, in this case, *k* represents the number of reference arrays contained in the database shown in Table **II**. Also, *r* represents the number of parameters contained in each array.

Step 2: The contained feature parameter ($\Lambda_{k,r}$) must be kept in the same data dimension, the normalized value is defined as $\Pi_{k,r}$, its formula is (**16**). Where, Λ_{raver} represents the average value of the feature parameter belonging to the same category.

$$\Pi_{k,r} = \frac{\Lambda_{k,r}}{\Lambda_{raver}}, \Lambda_{raver} = \frac{1}{22}\sum_{k=0}^{21}\Lambda_{k,r} \quad r \in [1,5] \tag{16}$$

Step 3: Calculating the deviation value between $\Lambda_{0,i}$ and $\Lambda_{k,i}$, respectively. The calculation results are defined as $\Delta_{k,i}$.

$$\Delta_{k,r} = \left|\Pi_{k,r} - \Pi_{0,r}\right|, k \in [1,21], r \in [1,5] \tag{17}$$

Step 4: Calculating the maximum (M_r) value minimum value (m_r) of the $\Delta_{k,r}$. of the parameters within the same category.

$$M_r = \max_k[\Delta_{k,r}] \tag{18}$$

$$m_r = \min_k[\Delta_{k,r}] \tag{19}$$

Step 5: Calculating the correlation coefficient $\gamma_{k,r}$ between the feature parameters $\Lambda_{0,r}$ and $\Lambda_{k,r}$ (k=1, 2, …, 21), respectively. The ξ is called the distinguishing coefficient, it is regarded as 0.5 in this work.

$$\gamma_{k,r} = \frac{m_r + \xi \cdot M_r}{\Delta_{k,r} + \xi \cdot M_r}, \quad k \in [1,21], r \in [1,5] \tag{20}$$

Step 6: Finally, calculating the correlation degree $\gamma_{k,r}$ (similarity) between the unknown samples and the known samples (shown in Table **III**), as is shown in (**21**). Therefore, the greater the correlation degree γ_k is, the closer the unknown sample to the known sample marked as k, and the moisture content corresponding to the known sample with the maximum value of γ_k can be regarded as the evaluation result.

$$\gamma_k = \frac{1}{5}\sum_{r=1}^{5}\gamma_{k,r}, \quad k \in [1,21], r \in [1,5] \tag{21}$$

B. Scheme for Moisture Evaluation of Oil-immersed Bushing

In order to prove the applicability and feasibility of the proposed method, in this section, three bushings installed in the 220 kV transformers are selected for performing the verification experiments. The scheme for field testing is plotted in Fig. **6**.

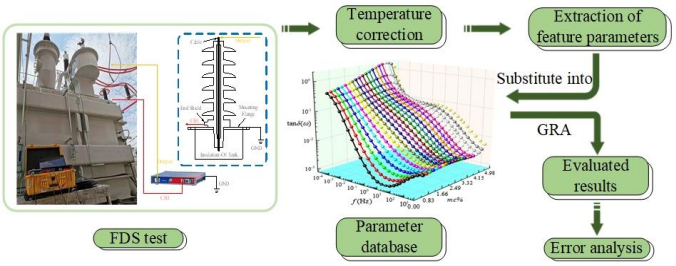

Fig. 6. The scheme for moisture evaluation of oil-immersed bushings under field conditions.

1) FDS measurement of the oil-immersed bushings

The connection diagram of the FDS test of the oil-immersed bushings is shown in Fig. **7**(a). Specifically, the output terminal (high voltage terminal) of the DIRANA is connected to the input terminal of the bushing. The CH1 (low voltage terminal) is connected to the end shield at the bottom of the bushing. To ensure the safety and reliability of the measurement, DIRANA and the flange of the bushing are required to ground well. Then, The FDS test results are shown in Fig. **7**(b).

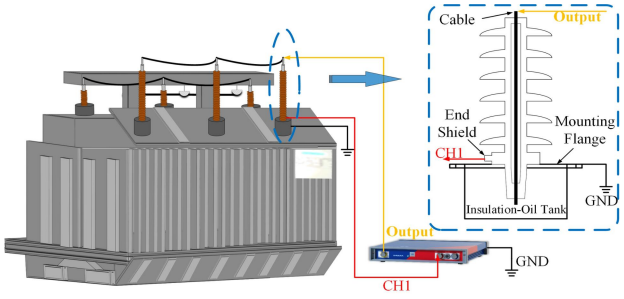

(a)

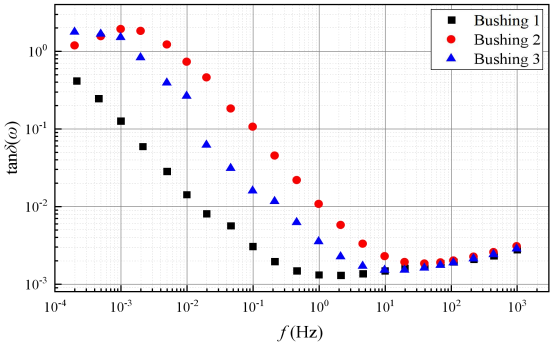

(b)

Fig. 7. The pictures about field testing. (a) Connection diagram of the FDS test, (b) The FDS test result of the oil-immersed bushings.

2) Correction of the temperature effect on FDS results

The temperature applied in FDS tests under lab conditions and maintains 45°C. Thus, both the feature parameters and even the constructed database are only available when the test temperature is 45°C (i.e. 318.15K). However, it is very difficult to maintain this temperature under field testing, the actual test temperatures of three bushings are sequentially equal to 298.15, 308.15, and 298.15K. Since the temperature impact could severely affect the FDS results, it is thus required to correct the temperature impact on the measured tan$\delta(\omega)$. By virtue of this, the extracted feature parameters of the tested bushings could also be suitable for the developed database (shown in Table **III**) when correction is completed.

One of the prevailing methods is so-called the 'master curve' technique, which originates from the Arrhenius theory [17]. The published results showed that the FDS curves measured at any test temperatures could be translated to a general curve corresponding to a uniform reference temperature by using the 'shift factor $\alpha(T)$'. The formula for calculating $\alpha(T)$ is shown in (**22**), then, by multiplying the measurement frequency by the $\alpha(T)$, the resulting curves are the corrected curve corresponding to the reference temperature, it is shown in (**23**) [9].

$$\alpha(T) = EXP[E_a(1/T_t - 1/T_{ref})/R] \tag{22}$$

$$f_{ref} = f_t \cdot \alpha(T) \tag{23}$$

Where, T_{ref} and T_t are the reference temperature (318.15K) and test temperature; f_t and f_{ref} are the frequency corresponding a point on the curve before and after multiplying the $\alpha(T)$; E_a is the activation energy of oil-immersed cellulose, which is assumed as 103 kJ/mol in this work [10]; and R is the gas constant (R=8.314 J/mol/K). Then, the calculated $\alpha(T)$ is sequentially equal to 13.6277, 3.5384, and 13.6277. The resulting tan$\delta(\omega)$ curves (after temperature correction) are thus obtained.

3) Extraction of feature parameters for characterizing the inside moisture

Due to the mentioned procedure, the tan$\delta(\omega)$ curves after temperature correction can be fitted by (**14**), by which the feature parameters for characterizing the inside moisture can be obtained. The comparison between the fitting curves and the corrected curves is plotted in Fig. **8**. It can be observed that two kinds of curves coincide in whole frequency regions. The contained feature parameters (Λ_i) are listed in Table **IV**, which could be applied for moisture evaluation.

Citation information: DOI: 10.17775/CSEEJPES.2021.00510, CSEE Journal of Power and Energy Systems

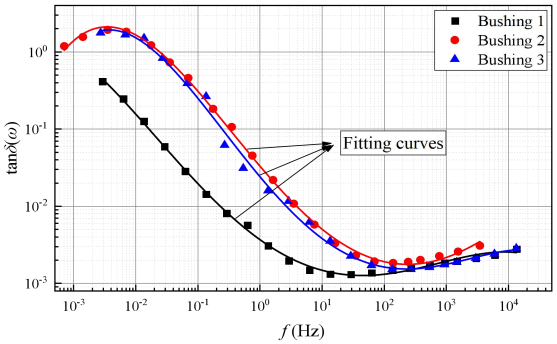

Fig. 8. The tan$\delta(\omega)$ curves of three bushings after temperature correction.

TABLE IV
THE EXTRACTED FEATURE PARAMETERS OF OIL-IMMERSED BUSHINGS

Label	Feature parameters					R^2
	Λ_0	Λ_1	Λ_2	Λ_3	Λ_4	
Bushing 1	-2.4359	-0.5776	0.1704	0.0144	-0.0059	0.998
Bushing 2	-1.4803	-0.94864	0.08352	0.0533	-0.00662	0.999
Bushing 3	-1.6173	-0.9655	0.1176	0.0554	-0.0099	0.996

C. *The evaluation results by using proposed method*

The GRA model is applied to calculate the correlation degree γ_i between the feature parameters of the known samples (in Table **III**) and the feature parameters of unknown samples (in Table **IV**). Then, the calculation results γ_k between the oil-immersed bushings and known samples are obtained and listed in Fig. **9**, respectively. Based on the principle that the higher the correlation, the more similar the condition.

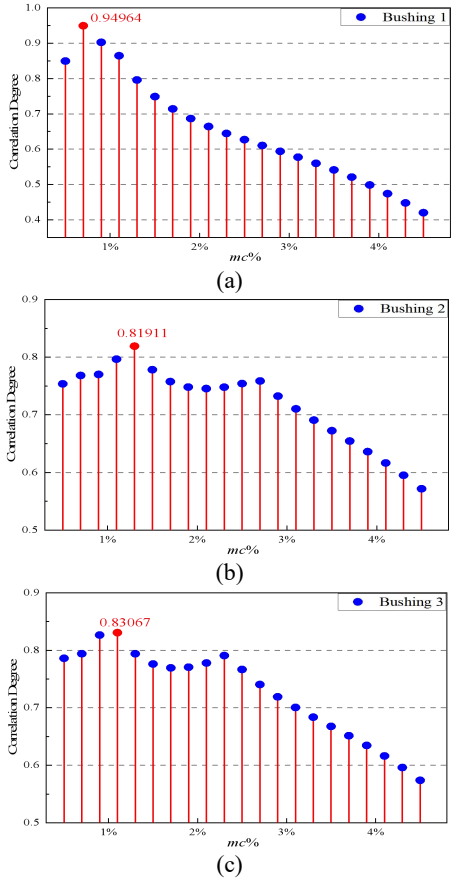

Fig. 9. Calculation results for the correlation degree.
(a) Bushing 1, (b) Bushing 2, (c) Bushing 3.

According to the calculation results shown in Fig. **9**, it is found that the feature parameters of the known sample marked 2 (in Table **III**) are closest to the tested bushing, in which the corresponding moisture is equal to 0.7 %. Similarly, the evaluated moisture of other bushings (Bushing 2 to 3) is equal to 1.3 % and 1.1 % according to the results of GRA.

Since the approximate moisture inside the insulation system can be obtained by using DIRANA when collecting the FDS data. Thus, in order to prove the accuracy of the evaluated results. The internal software of DIRANA is used to test the moisture of the whole oil-paper system in the bushing. Nevertheless, the research object of DIRANA is the moisture inside the insulation system rather than the paper insulation.

Thus, if the moisture obtained by using the DIRANA and the proposed method is similar, the damp conditions of the tested equipment can be judged. Otherwise, another approach (such as KFT) should be involved to decide by synthetically considering the results collected by DIRANA and the proposed method. Then, the comparison between the evaluated results (by using the proposed model) and the tested results (by using DIRANA) is shown in Table **V**.

TABLE V
THE COMPARISON BETWEEN THE EVALUATED RESULTS AND THE ANALYZED RESULTS

Label	Tested *mc*%	Evaluated *mc*%	*RE*	*AE*
Bushing 1	0.6 %	0.7 %	16.67 %	0.1 %
Bushing 2	1.6 %	1.3 %	18.75 %	0.3 %
Bushing 3	1.2 %	1.1 %	8.33 %	0.1 %

Where, a quantitative error analysis between the evaluated results and the analyzed result is employed to prove its reliability. Equation (**24**) and (**25**) is used to calculate the relative error (*RE*) and absolute error between the evaluated *mc%* and the tested *mc%*. Also, from Table **V**, the average value of *RE* (*AE*) of the three bushings is 14.6 % (0.17 %), which is acceptable. Thus, the feasibility and accuracy of the proposed method when applying it in field testing are preliminarily verified.

$$RE = \frac{\left|\text{Tested } mc\%\text{-Evaluated } mc\%\right|}{\text{Tested } mc\%} \times 100\% \tag{24}$$

$$AE = \left|\text{Tested } mc\%\text{-Evaluated } mc\%\right| \tag{25}$$

V. CONCLUSION

In this paper, tan$\delta(\omega)$ curves of oil-immersed cellulose samples with various moisture are measured in laboratory conditions, and the feature parameters were extracted by Taylor series model to characterize the inside moisture, then, a database is established to provide the data basis for moisture evaluation when combining the GRA. The accuracy and feasibility of the proposed method were verified by using three oil-immersed bushings in field conditions. The present findings have led to the following conclusions.

i. The tan$\delta(\omega)$ curves of oil-immersed cellulose samples with various moisture can be well fitted by using the Taylor series model to access the feature parameters, in which the obtained fitting results begin to meet the requirement of accuracy when the corresponding order is close to 4.
ii. It is found that an obvious variation rule between the extracted feature parameters and moisture, has been

proved by using the fitting analysis. Also, the related quantitative equations were obtained and further used to form a feature parameter database.

iii. By combining the feature parameter database and GRA, the moisture inside the selected bushings can be readily evaluated. The results showed that the average relative error of the evaluation results is less than 14.6 %, which preliminarily proved that the method could be feasible when working under field conditions.

REFERENCES

[1] J. Y. Wang, R. J. Liao, Y. Y. Zhang, F. J. Meng, "Economic Life Assessment of Power Transformers Using an Improved Model," *CSEE J. Power Energy*, vol. 1, no. 3, pp. 68-75, Sep. 2015.

[2] W. L. Liao, D. C. Yang, Y. S. Wang, X. Ren, "Fault diagnosis of power transformers using graph convolutional network," *CSEE J. Power Energy*, vol. 7, no. 2, pp. 241-249, Sep. 2021.

[3] A. Mikulecky and Z. Stih, "Influence of Temperature, Moisture Content and Ageing on Oil Impregnated Paper Bushings Insulation," *IEEE Trans. Dielectr. Electr. Insul.*, vol. 20, no. 4, pp. 1421-1427, Aug. 2013.

[4] M. Kes and B. E. Christensen, "Degradation of cellulosic insulation in power transformers: a SEC-MALLS study of artificially aged transformer papers," *Cellulose*, vol. 20, no. 4, pp. 2003-2011, Aug. 2013.

[5] O. H. Arroyo, J. Jalbert, I. Fofana and M. Ryadi, "Temperature dependence of methanol and the tensile strength of insulation paper: kinetics of the changes of mechanical properties during ageing," *Cellulose*, vol. 24, no. 2, pp. 1031-1039, Feb. 2017.

[6] R. J. Liao, Y. Y. Du, L. J. Yang and J. Gao, "Quantitative diagnosis of moisture content in oil-paper condenser bushing insulation based on frequency domain spectroscopy and polarisation and depolarisation current," *IET Gener. Transm. Distrib.*, vol. 11, no. 6, pp. 1420-1426, Apr. 2017.

[7] J. Jalbert, E. Rodriguez-Celis, S. Duchesne, B. Morin, M. Ryadi and R. Gilbert, "Kinetics of the production of chain-end groups and methanol from the depolymerization of cellulose during the ageing of paper/oil systems. Part 3: extension of the study under temperature conditions over 120 degrees C," *Cellulose*, vol. 22, no. 1, pp. 829-848, Feb. 2015.

[8] D. N. Zhang, H. X. Zhao, H. Yun, X. W. Liu, Y. H. Han, H. B. Mu and G. J. Zhang, "Study on FDS characteristics of oil-immersed paper insulation bushing under non-uniform moisture content," *IET Sci. Meas. Technol.*, vol. 12, no. 5, pp. 691-697, Aug. 2018.

[9] J. F. Liu, X. H. Fan, Y. Y. Zhang, H. B. Zheng and J. Jiao, "Temperature correction to dielectric modulus and activation energy prediction of oil-immersed cellulose insulation," *IEEE Trans. Dielectr. Electr. Insul.*, vol. 27, no. 3, pp. 956-963, Jun. 2020.

[10] J. F. Liu, X. H. Fan, Y. Y. Zhang, C. H. Zhang, Z. X. Wang, "Aging evaluation and moisture prediction of oil-immersed cellulose insulation in field transformer using frequency domain spectroscopy and aging kinetics model," *Cellulose*, vol. 27, no. 12, pp. 7175-7189, Aug. 2020.

[11] A. M. Emsley, "Kinetics and mechanisms of the low-temperature degradation of cellulose," *Cellulose*, vol. 1, pp. 26-56, Mar. 1994.

[12] A. M. Emsley, R. J. Heywood, M. Ali and C. M. Eley, "On the kinetics of degradation of cellulose," *Cellulose*, vol. 4, no. 1, pp. 1-5, Mar. 1997.

[13] M. M. Islam, G. Lee, S. N. Hettiwatte, "A review of condition monitoring techniques and diagnostic tests for lifetime estimation of power transformers," *Electr. Eng.*, vol. 100, pp. 581–605, 2018.

[14] P. Werelius, M. Ohlen, C. Jialu and D. M. Robalino, "Dielectric frequency response measurements and dissipation factor temperature dependence," in *Proc. ELINSL*, San Juan, USA, 2012, pp. 296-300, Jun. 2012.

[15] G. Lu and P. J. Zhang, "A novel leakage-current-based online insulation monitoring strategy for converter transformers using common-mode and differential-mode harmonics in VSC system," *IEEE Trans. Ind. Electron.*, vol. 68, no. 2, pp. 1636–1645, Feb. 2021.

[16] P. Żukowski, T. N. Kołtunowicz, K. Kierczyński, P. Rogalski, J. Subocz, M. Szrot, M. Gutten, M. Sebok and D. Korenciak, "Dielectric losses in the composite cellulose–mineral oil–water nanoparticles: theoretical assumptions," *Cellulose*, vol. 23, no. 3, pp. 1609-1616, Apr. 2016.

[17] L. J. Zhou, D. Y. Wang, Y. Cui, L. Q. Zhang, L. J. Wang, L. Guo, "A Method for Diagnosing the State of Insulation Paper in Traction Transformer Based on FDS Test and CS-DQ Algorithm," *IEEE Trans. Transport. Electrific.*, vol. 7, no. 1, pp. 91-103, Mar. 2021.

[18] A. Setayeshmehr, I. Fofana, C. Eichler, A. Akbari, H. Borsi and E. Gockenbach, "Dielectric spectroscopic measurements on transformer oil-paper insulation under controlled laboratory conditions," *IEEE Trans. Dielectr. Electr. Insul.*, vol. 15, no. 4, pp. 1100-1111, Aug. 2008.

[19] C. Wei, C. B. Liao, Y. C. Lu, L. Du and X. X. Chen, "Influence of Moisture on Dielectric Responses of Oil-Impregnated Paper Condenser Bushings," *Proc. ICEPE-ST*, Kitakyushu, Japan, pp. 709-712, Oct. 2019.

[20] D. N. Zhang, H. Yun, J. Y. Zhan, X. Sun, W. L. He, C. B. Niu, H. B. Mu and G. J. Zhang, "Insulation Condition` Diagnosis of Oil-Immersed Paper Insulation Based on Non-linear Frequency-Domain Dielectric Response," *IEEE Trans. Dielectr. Electr. Insul.*, vol. 25, no. 5, pp. 1980-1988, Oct. 2018.

[21] N. Baruah, S. K. Nayak and S. K. Pratihar, "Quantitative Effect of Aging Duration on Dielectric Parameters Based on Frequency Response," *IEEE Trans. Instrum. Meas.*, vol. 71, pp. 1-9, Nov. 2022.

[22] J. Gao, L. J. Yang, Y. Y. Wang, X. Liu, Y. D. Lv, and H. B. Zheng, "Condition diagnosis of transformer oil-paper insulation using dielectric response fingerprint characteristics," *IEEE Trans. Dielectr. Electr. Insul*, vol. 23, no. 2, pp. 1207-1218, Apr. 2016.

[23] J. P. Allouche, M. Mendès France, "Hadamard grade of power series," *J. Number Theory*, vol. 131, no. 11, pp. 2013-2022, Nov. 2011.

[24] J. F. Liu, X. H. Fan, Y. Y. Zhang, S. Li and J. Jiao, "Frequency Domain Spectroscopy Prediction of Oil-Immersed Cellulose Insulation under Diverse Temperature and Moisture," *IEEE Trans. Dielectr. Electr. Insul.* vol. 27, no. 6, pp. 1820-1828, Dec. 2020.

[25] J. F. Liu, S. C. Yang, Y. Y. Zhang, H. Zheng, Z. Shi and C. H. Zhang, "A modified X-model of the oil-impregnated bushing including non-uniform thermal aging of cellulose insulation," *Cellulose*, vol. 27, no. 8, pp. 4525-4538, May 2020.